Supporting information

Systematic exploration of alkali–anion pairs for descriptor identification on OH-mediated methane coupling

Shintaro Yoshida, William J. Movick, Keisuke Obata and Kazuhiro Takanabe*

Department of Chemical System Engineering, School of Engineering,
The University of Tokyo, 7-3-1 Hongo, Bunkyo-ku, Tokyo, Japan.
Corresponding author: Kazuhiro Takanabe takanabe@chemsys.t.u-tokyo.ac.jp

Experimental

1.1 Catalyst preparation

Most SiO_2-supported catalysts were prepared by impregnation methods. $Na_2WO_4\cdot 2H_2O$ (Sigma-Aldrich), $Na_2MoO_4\cdot 12H_2O$ (Sigma-Aldrich), Na_2CO_3 (Sigma-Aldrich), $Na_3PO_4\cdot 12H_2O$ (Sigma-Aldrich), Na_2SO_4 (Wako), K_2WO_4 (Alfa Aesar), K_2MoO_4 (Sigma-Aldrich), K_2CO_3 (Sigma-Aldrich), K_3PO_4 (Sigma-Aldrich), K_2SO_4 (Sigma-Aldrich). Li_2WO_4 (Alfa Aesar), Li_2MoO_4 (Alfa Aesar), Li_2CO_3 (Sigma-Aldrich), Li_3PO_4 (Sigma-Aldrich), Li_2SO_4 (Sigma-Aldrich), Cs_2WO_4, Cs_2CO_3 (Wako), and $Cs_2SO_4\cdot H_2O$ (Wako) were used for the supported materials and SiO_2 (Silica Gel Grade 643, Sigma-Aldrich) was used for the support. The required amount of each supported material was dissolved in 5 ml of deionized water, and then, the solution was stirred with SiO_2 to achieve 5 wt % supported material and a total of 1 g of the whole sample. The samples were dried in ambient air at 130 °C for 5 h and the treated in ambient air with a ramp rate of 10 °C min^{-1} and held at 900 °C for 8 h. For preparation of 5 wt% Cs_2MoO_4/SiO_2 and 5 wt% Cs_3PO_4/SiO_2, stoichiometric amount of $CsNO_3$ (Wako), H_2MoO_4 (Sigma-Aldrich) and $NH_4H_2PO_4$ (Sigma-Aldrich) were used as precursor instead.

The OCM rates and selectivity were measured in a U-shape quartz flow reactor with 4 mm of inner diameter. Catalysts were packed and held in U-shaped reactor tube by plugs of quartz wool. Those were located in the second half of the reactor to minimize secondary reaction. The reaction temperature was controlled by an electric furnace and Omron controller (Omron, ESCC), and the temperature was measured with a K-type thermocouple at the outer surface of the reactor closest to the catalyst bed. For reaction tests, CH_4 (>99.999%) and O_2 (20.0%, diluted by Ar) were used as reactants, and Ar (>99.9999%) was used as a diluent.

The flow was controlled by mass flow controllers (Brooks, SLA5850S). A saturator with a temperature- controlled water jacket (15 °C) was used to introduce H_2O to the reactant feed. The concentration of reactants and products was measured using a GC (Shimazu, GC-2014) gas chromatograph with an Rt- Molsieve 5A capillary column (0.25 mm, 10 m, Backflush 1.0 µL) and an Rt-Q-bond capillary column (0.25 mm, 3 m) with a thermal conductivity detector and an RT-Q-bond capillary column (0.25 mm, 12 m) with a thermal conductivity detector. In our experiment, CH_4, C_2H_2, C_2H_4, C_2H_6, C_3H_6, C_3H_8 and C_4H_8 were measured by GC-FID and CH_4, O_2, H_2, CO and CO_2 were measured by GC-TCD. CH_4 conversion, product selectivity, and yield were calculated by eqs 1−3.

$$\mathrm{CH_4\ conversion\ (\%)} = \frac{\text{moles of carbon in all products}}{\text{moles of carbon in all products and unreacted } \mathrm{CH_4}} \times 100$$

$$\text{Selectivity (\%)} = \frac{\text{total moles of carbon in specific product}}{\text{total moles of carbon in all products}} \times 100$$

$$\text{Yield} = \frac{\text{CH}_4\ \text{conversion (\%)} \times \text{selectivity (\%)}}{100}$$

To minimize the effects of product formation in our kinetic analysis, the CH_4 conversion rate was measured at below 5% conversion and extrapolated to 1% conversion.

To minimize the effects of product formation in our kinetic analysis, the CH_4 conversion rate was measured at below 5% conversion and extrapolated to 1% conversion.

Table S1

The OCM detailed yield and selectivity of WO_4-related catalysts taken at 850°C at wet condition (10 kPa CH_4 and 0.9-10 kPa O_2 with an additional 1.7 kPa H_2O feed, 30 ml min^{-1} of total flow rate)

Catalysts	**Catalyst amount / mg**	**CH_4/O_2 ratio**	**CH_4 conv. /%**	**C_{2+} sel. /%**	**Selectivity**					
					C_2H_6	C_2H_4	C_2H_2	C_{3+}	CO	CO_2
Li_2WO_4/SiO_2	0.5	12	9.4	0.63	4.9	1.7	0	0	71	22
	0.5	9	11	0.93	5.8	2.5	0	0	69	23
	0.5	6	15	1.6	6.3	3.9	0.06	0.11	65	24
	0.5	3	28	3.2	5.2	6.2	0.10	0.21	62	26
	0.5	2	41	4.5	3.8	7.1	0.12	0.27	60	28
	0.5	1	69	4.8	1.4	5.5	0.11	0.19	58	35
Na_2WO_4/SiO_2	0.6	12	14	11	40	39	N.M.	2.5	7.2	11
	0.6	9	16	13	36	42	N.M.	3.5	7.6	12
	0.6	6	23	17	29	45	N.M.	3.6	9.2	14
	0.6	3	38	24	17	44	N.M.	4.3	14	20
	0.6	2	50	26	12	41	N.M.	3.6	18	26
	0.6	1	80	25	4.9	27	N.M.	1.7	26	41
K_2WO_4/SiO_2	0.8	12	13	10	35	45	N.M.	0	9.4	11
	0.8	9	15	12	32	47	N.M.	0	10	12
	0.8	6	21	16	24	47	N.M.	3.8	12	14
	0.8	3	35	23	15	44	N.M.	3.9	17	20
	0.8	2	45	25	10	39	N.M.	3.2	22	26
	0.8	1	71	24	4.3	25	N.M.	1.6	31	39
Cs_2WO_4/SiO_2	0.8	12	15	11	29	41	0.61	4.9	8.0	17
	0.8	9	18	13	27	43	0.64	4.6	8.3	17
	0.8	6	23	16	21	44	0.65	5.0	9.8	20
	0.8	3	36	21	13	39	0.58	5.0	14	29
	0.8	2	48	22	8.1	33	0.50	4.3	17	37
	0.8	1	71	18	3.5	19	0.51	2.3	21	54

Table S2

The OCM detailed selectivity and rate of various catalysts taken at 850 °C at dry and wet conditions.

Catalysts	**C_2 sel. (dry)**	**C_2 sel. (wet)**	**r_{dry}[a]**	**r_{wet}[b]**	**Ratio (r_{dry}/r_{wet})**	**BET surface area / $m^2\ g^{-1}$**	**Catalyst loading[c] / wt% (AAS / ICP)**	**Selectivity (S_{dry} / S_{wet})**						
								C_2H_6	C_2H_4	CO	C_2H_2	C_3H_8	C_3H_6	CO_2
Li_2WO_4/SiO_2	42	61	1.4	3.2	2.3	4.7	1.7 : 2	38.0 / 53.4	3.0 / 5.9	49.5 / 34.8	0.0 / 0.2	0.0 / 0.1	0.0 / 0.1	9.4 / 5.5
Li_2MoO_4/SiO_2	48	63	0.87	4.4	2.9	1.0	3.9 : 3.9	44.6 / 54.9	2.8 / 7.3	19.1 / 17.6	0 / 0.0	0.0 / 0.3	0 / 0.1	33.4 / 19.8
Li_3PO_4/SiO_2	13	45	4.2	4.4	1.0	32	3.4 : 4.5	11.9 / 39.5	1.0 / 7.1	87.4 / 53.7	0.0 / 0.0	0 / 0.0	0 / 0.0	0 / 0
Li_2SO_4/SiO_2	49	68	0.30	0.34	1.2	2.4	3.8 : 4.2	44.9 / 62.6	3.9 / 6.2	42.1 / 31.1	0 / 0	0 / 0	0.0 / 0.1	9.0 / 0
Li_2CO_3/SiO_2	39	65	0.30	0.70	2.3	1.5	0.52 : 1	35.7 / 58.1	3.2 / 5.5	49.7 / 29.1	0 / 0	0 / 0	0 / 0.0	11.3 / 7.2
Na_2WO_4/SiO_2	80	91	0.72	2.4	3.3	2.5	– : 5	73.3 / 84.0	6.9 / 6.3	14.9 / 6.7	0.0 / 0	0.1 / 0.2	0.1 / 0	4.7 / 2.9
Na_2MoO_4/SiO_2	45	68	0.79	1.8	2.1	1.8	– : 3.5	41.4 / 61.2	3.8 / 5.0	31.5 / 20.2	0 / 0	0 / 0.1	0 / 0.0	23.2 / 13.5
Na_3PO_4/SiO_2	51	67	0.84	1.2	1.4	1.4	– : 3	47.1 / 61.0	4.3 / 5.5	42.2 / 29.7	0 / 0	0 / 0.1	0.0 / 0.1	6.4 / 3.6
Na_2SO_4/SiO_2	51	60	0.52	0.66	1.3	15	– : 4.3	45.9 / 55.0	5.0 / 5.3	43.4 / 35.7	0 / 0	0 / 0	0 / 0	5.7 / 4.0
Na_2CO_3/SiO_2	45	57	0.17	0.20	1.2	0.65	– : 2.3	32.8 / 41.3	12.3 / 15.9	54.9 / 42.8	0 / 0	0 / 0	0 / 0	0 / 0
K_2WO_4/SiO_2	76	89	0.68	1.9	2.8	2.7	3.8 : 9	71.2 / 81.7	5.9 / 7.7	14.8 / 6.9	N.M. / N.M.	0 / 0	0 / 0	8.1 / 3.6
K_2MoO_4/SiO_2	38	53	0.40	1.0	2.5	2.1	3.1 : 5	35.8 / 49.0	1.8 / 3.9	47.0 / 37.4	N,M. / N,M.	0 / 0	0 / 0	15.4 / 9.8
K_3PO_4/SiO_2	76	88	0.24	0.44	1.8	0.96	3.6 : 8.6	57.8 / 68.9	22.8 / 9.2	19.4 / 21.9	N.M. / N.M.	0 / 0	0 / 0	0 / 0
K_2SO_4/SiO_2	68	77	0.12	0.16	1.3	21	0.47 : 0.9	60.7 / 69.9	7.4 / 6.5	29.1 / 21.9	N.M. / N.M.	0 / 0	0 / 0	2.7 / 1.6
K_2CO_3/SiO_2	64	69	0.068	0.054	0.79	1.1	2.3 : 6.3	51.5 / 53.1	12.4 / 16.3	36.1 / 30.7	N,M. / N,M.	0 / 0	0 / 0	0 / 0
Cs_2WO_4/SiO_2	68	87	0.75	1.7	2.3	5.4	2.7 : –	67.7 / 71.7	6.2 / 6.9	21.7 / 16.6	0.0 / 0	0.2 / 0.2	0.0 / 0	4.1 / 4.6
Cs_2MoO_4/SiO_2	25	46	1.6	2.4	1.5	1.4	2.2 : –	22.7 / 41.1	1.1 / 3.6	35.5 / 32.1	0 / 0.1	0 / 0.2	0 / 0	40.8 / 23.1
Cs_3PO_4/SiO_2	62	74	0.80	1.7	2.1	1.9	2.9 : –	57.1 / 66.7	4.7 / 6.0	36.9 / 26.7	0 / 0	0.0 / 0.2	0 / 0	1.3 / 0.6
Cs_2SO_4/SiO_2	42	53	0.042	0.050	1.2	26	4.2 : –	29.1 / 41.2	8.1 / 12.7	62.8 / 46.1	0 / 0	0 / 0	0 / 0	0 / 0
Cs_2CO_3/SiO_2	50	57	0.38	0.45	1.2	0.53	0.94 : –	41.3 / 46.5	8.4 / 9.5	45.6 / 37.8	0 / 0.5	0 / 0	0 / 0.6	4.8 / 5.0

a) Taken at 1% CH_4 conversion with 10 kPa CH_4 and 1.7 kPa O_2 at 850 °C.

b) Same as a) but with an additional 1.7 kPa H_2O feed.

c) Determined from the alkali metal content measured from either atomic adsorption spectroscopy (AAS) or inductively coupled plasma (ICP) spectroscopy.

Table S3

Surface area and element analysis of alkali metal salt catalysts.

Catalyst	**BET surface area / $m^2\ g^{-1}$**	**Catalyst loading / wt% (AAS : ICP)**
Li_2WO_4/SiO_2	4.7	1.7 : 2.0
Li_2MoO_4/SiO_2	1.0	3.9 : 3.9
Li_3PO_4/SiO_2	32	3.4 : 4.5
Li_2SO_4/SiO_2	2.4	3.8 : 4.2
Li_2CO_3/SiO_2	1.5	0.52 : 1.0
Na_2WO_4/SiO_2	2.5	− : 5.0
Na_2MoO_4/SiO_2	1.8	− : 3.5
Na_3PO_4/SiO_2	1.4	− : 3.0
Na_2SO_4/SiO_2	15	− : 4.3
Na_2CO_3/SiO_2	0.7	− : 2.3
K_2WO_4/SiO_2	2.7	3.8 : 9.0
K_2MoO_4/SiO_2	2.1	3.1 : 5.0
K_3PO_4/SiO_2	1.0	3.6 : 8.6
K_2SO_4/SiO_2	21	0.47 : 0.90
K_2CO_3/SiO_2	1.1	2.3 : 6.3
Cs_2WO_4/SiO_2	5.4	2.7 : −
Cs_2MoO_4/SiO_2	1.4	2.2 : −
Cs_3PO_4/SiO_2	1.9	2.9 : −
Cs_2SO_4/SiO_2	26	4.2 : −
Cs_2CO_3/SiO_2	0.53	0.94 : −

Table S4

Assignment of SiO_2 crystal phase for each catalyst based on XRD results.

SiO_2 structure	**Catalyst**
Cristobalite	Li_2WO_4, Li_2SO_4, Na_2WO_4, Na_2MoO_4, Na_3PO_4, Na_2SO_4, Na_2CO_3, K_2WO_4, K_2MoO_4, K_3PO_4, K_2CO_3, Cs_2WO_4, Cs_2MoO_4, Cs_2SO_4, Cs_2CO_3
Tridymite	Li_2SO_4, Na_3PO_4, K_2CO_3
Quartz	Li_2MoO_4, Li_2SO_4, Li_2CO_3
Amorphous	Li_3PO_4, K_2SO_4, Cs_3PO_4

The polarizability of WO_4^{2-} and MoO_4^{2-} was obtained from reported dielectric factors ε_r. The reported ε_r for various materials was obtained and is shown in Table S5. The material polarizability can be calculated by using the Clausius-Mossotti equation:

$$A = \frac{3V}{4\pi}\frac{(\varepsilon_r - 1)}{(\varepsilon_r + 2)}$$

where V is the molar volume of the material. To estimate the polarizability of the anion, the following equation was applied[1]:

$$A(\text{total}) = A(MO_4^{2-}) + 2A(A^+)$$

Where $A(MO_4^{2-})$ is the polarizability of the anion and $A(A^+)$ is the polarizability of the alkali metal cation. Tabulated values for the polarizability of Li^+ and Na^+ were obtained from Coker[2] and gave 0.028 and 0.14 $Å^{-3}$, respectively. The calculated values for the anion polarizability are shown also in Table S2. Using this estimation, there is relatively good agreement in the case of WO_4^{2-} of around ~10 $Å^{-3}$. The estimated polarizability of MoO_4^{2-} took on a wider range of values. It is more likely those estimated from Li_2MoO_4 are closer to the real value as the low Li^+ polarizability should impact the calculation less than Na^+. However, it is clear from the values shown that the order of polarizability is $WO_4^{2-} > MoO_4^{2-} > PO_4^{3-} > SO_4^{2-}$.

Table S5

Estimated values of anion polarizability based on calculations of various materials

Material	ε_r	Reference	Calculated anion polarizability / Å^{-3}
Li_2MoO_4	5.5	Zhou et al.[3]	8.1
Li_2MoO_4	5.1	Kähäri[4]	7.8
Li_2MoO_4	5.5	Li et al.[5]	8.1
Li_2MoO_4	5.58	Zhang et al.[6]	8.1
Na_2MoO_4	4.31	Abbas et al.[7]	6.5
Na_2MoO_4	4.43	Gupta et al.[1]	6.7
Li_2WO_4	5.5	Zhen et al.[9]	10
Li_2WO_4	5.5	Zhou et al.[9]	10
Na_2WO_4	5.6	Yuan et al.[10]	9.9
Na_2WO_4	5.7	Hao et al.[11]	10

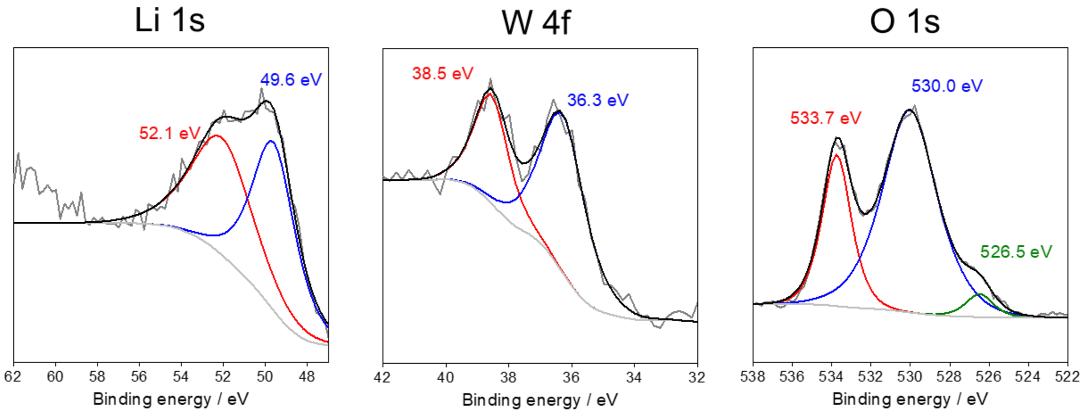

Figure S1. XPS spectra of Li_2WO_4/SiO_2

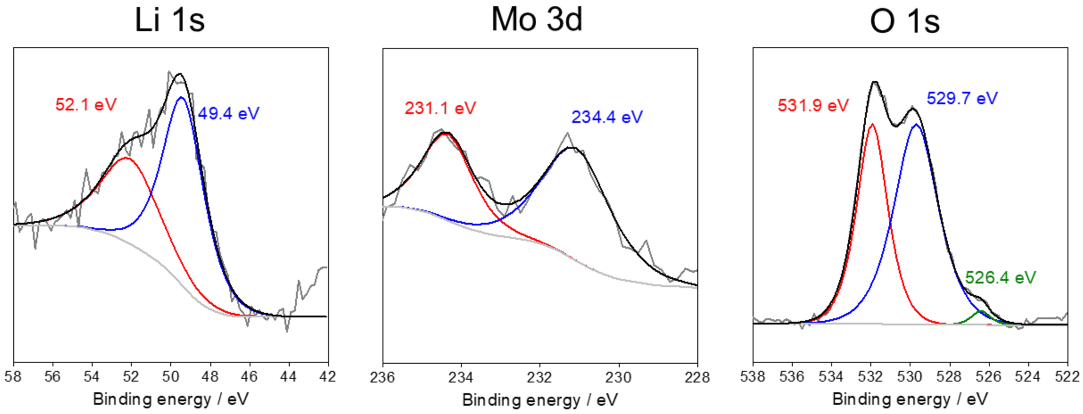

Figure S2. XPS spectra of Li_2MoO_4/SiO_2

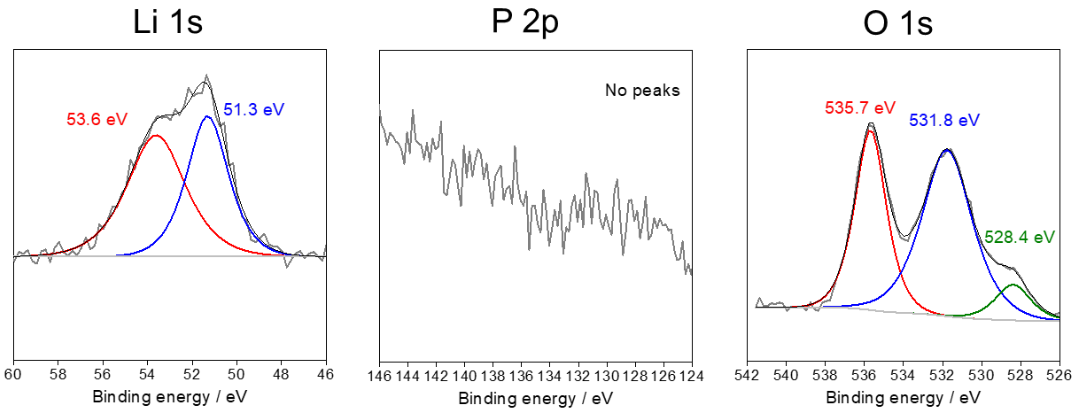

Figure S3. XPS spectra of Li_3PO_4/SiO_2

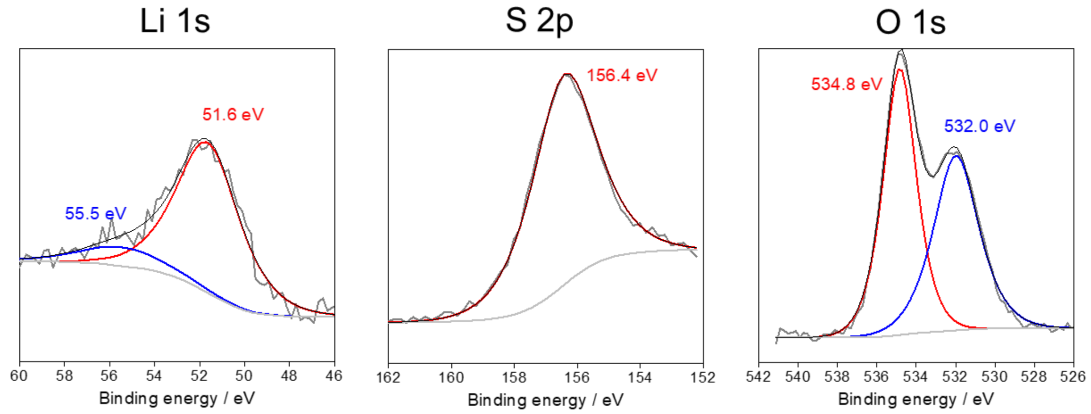

Figure S4. XPS spectra of Li_2SO_4/SiO_2

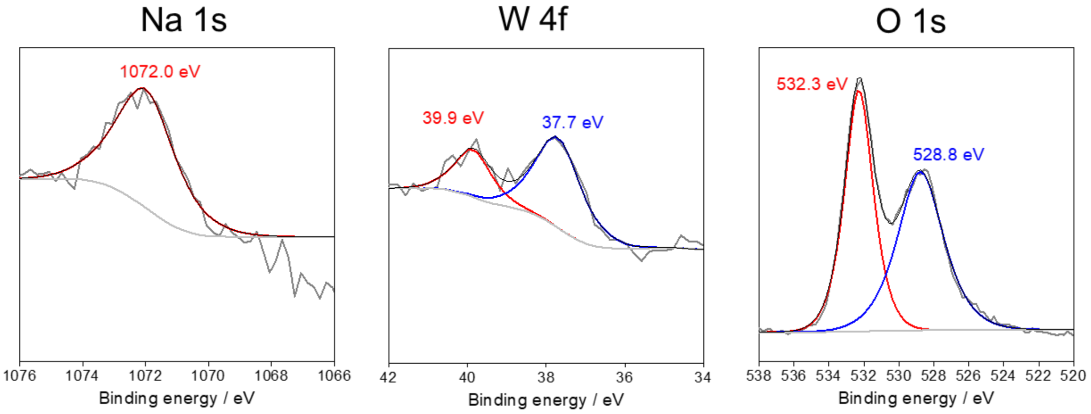

Figure S5. XPS spectra of Na_2WO_4/SiO_2

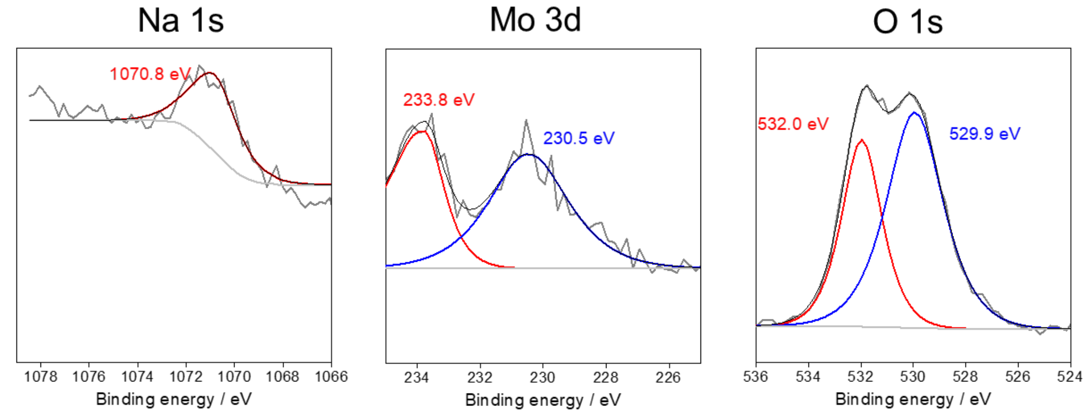

Figure S6. XPS spectra of Na_2MoO_4/SiO_2

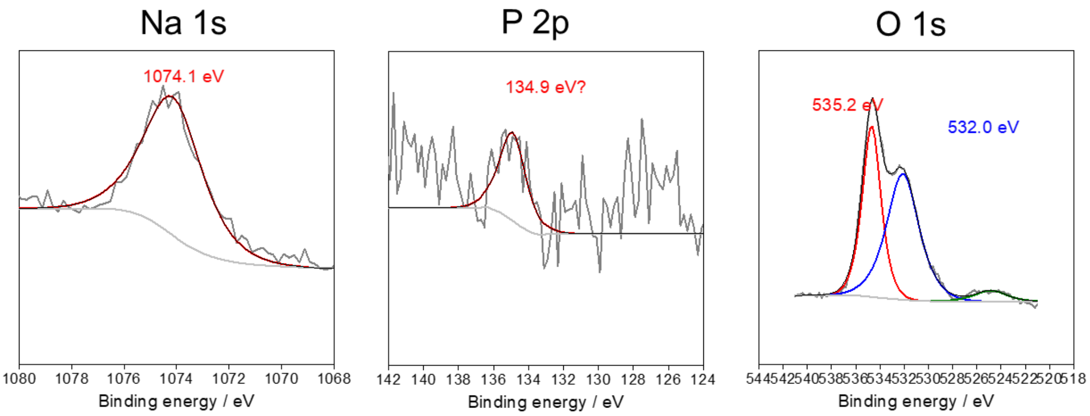

Figure S7. XPS spectra of Na_3PO_4/SiO_2

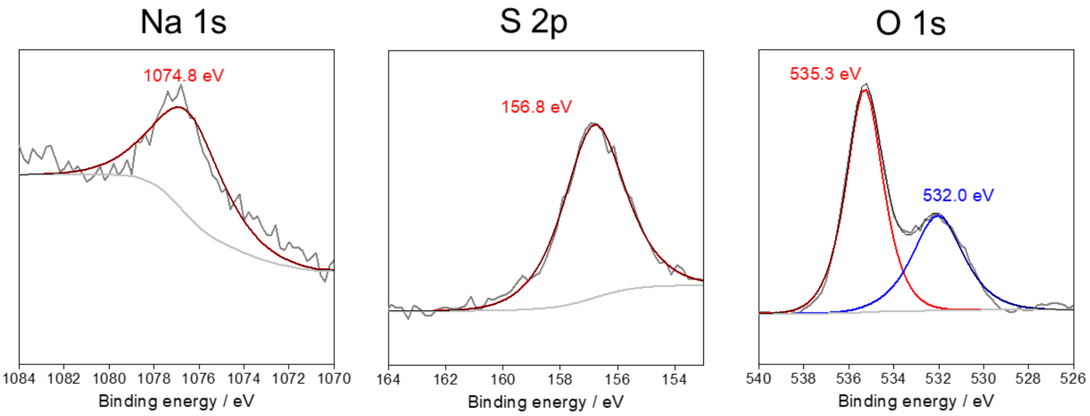

Figure S8. XPS spectra of Na_2SO_4/SiO_2

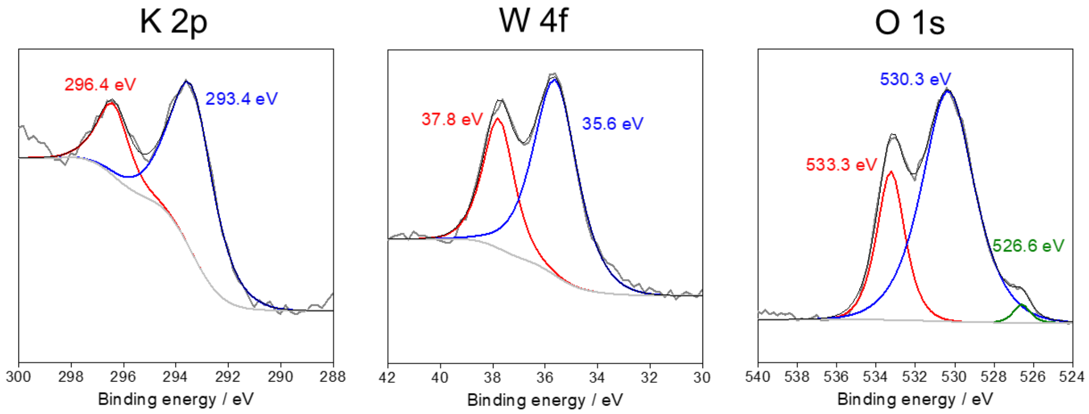

Figure S9. XPS spectra of K_2WO_4/SiO_2

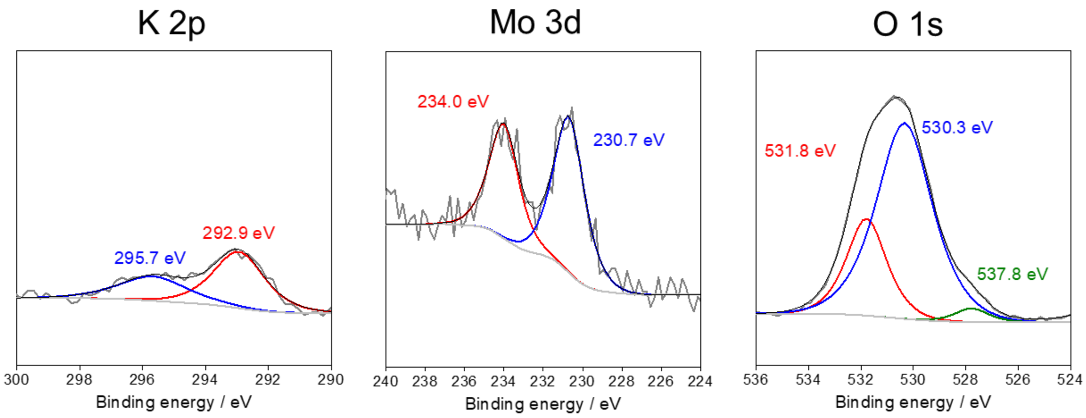

Figure S10. XPS spectra of K_2MoO_4/SiO_2

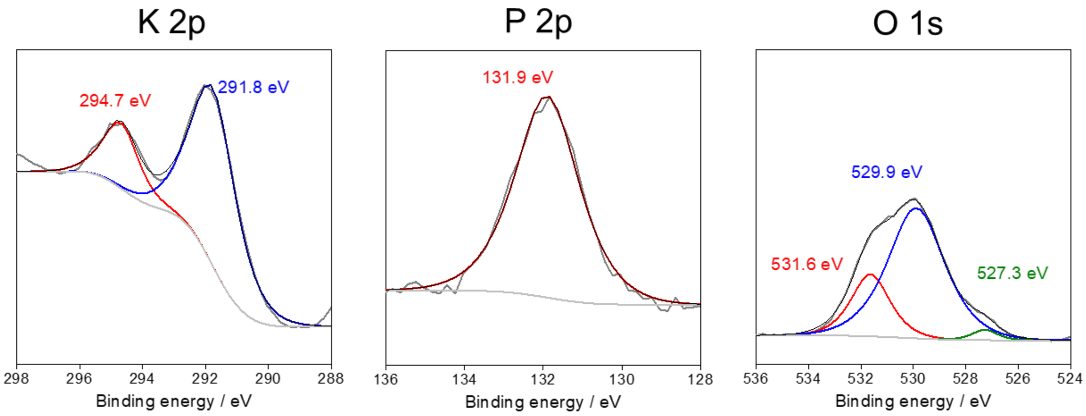

Figure S11. XPS spectra of K_3PO_4/SiO_2

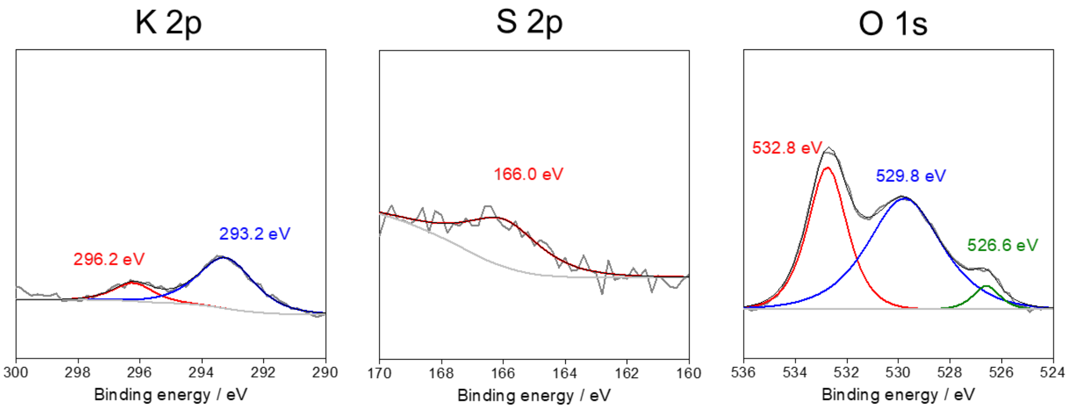

Figure S12. XPS spectra of K_2SO_4/SiO_2

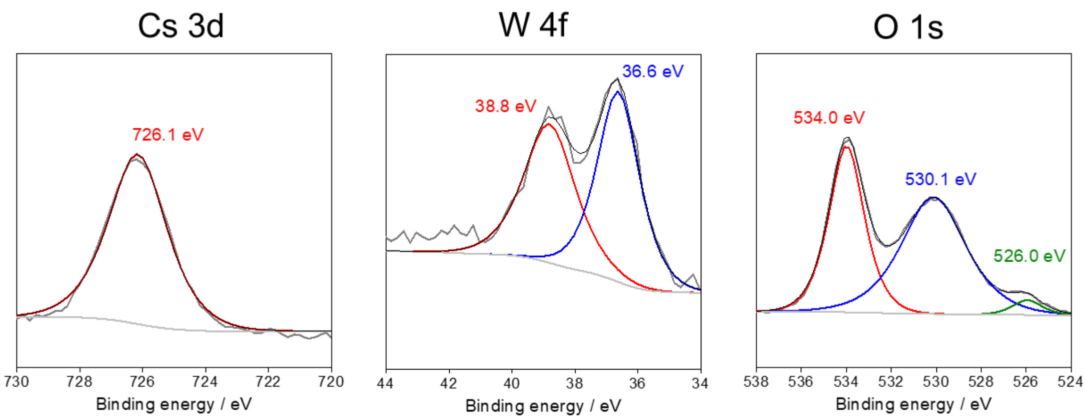

Figure S13. XPS spectra of Cs_2WO_4/SiO_2

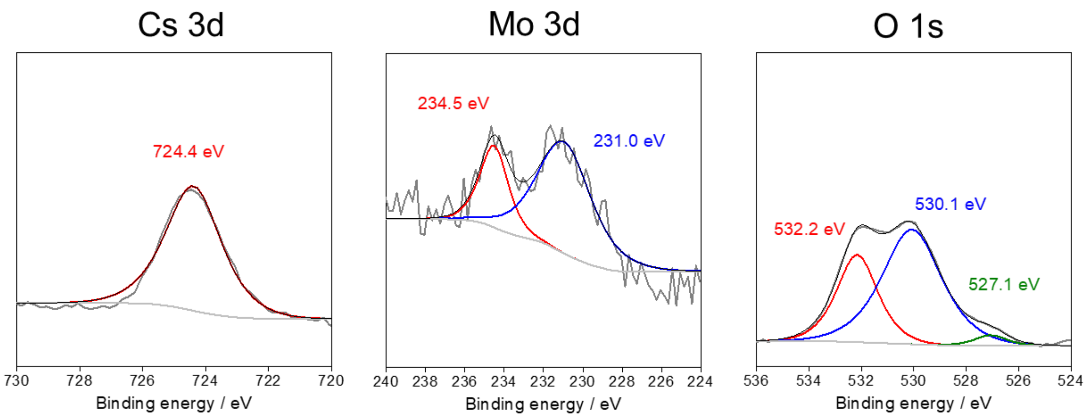

Figure S14. XPS spectra of Cs_2MoO_4/SiO_2

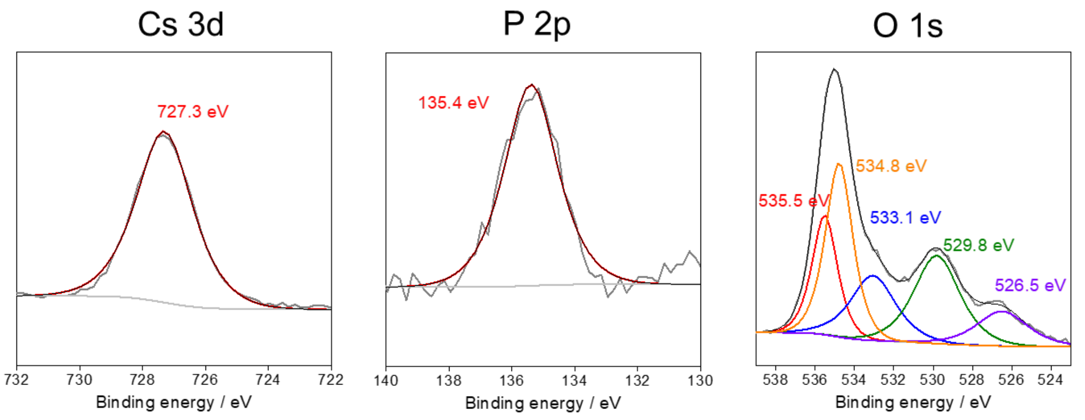

Figure S15. XPS spectra of Cs_3PO_4/SiO_2

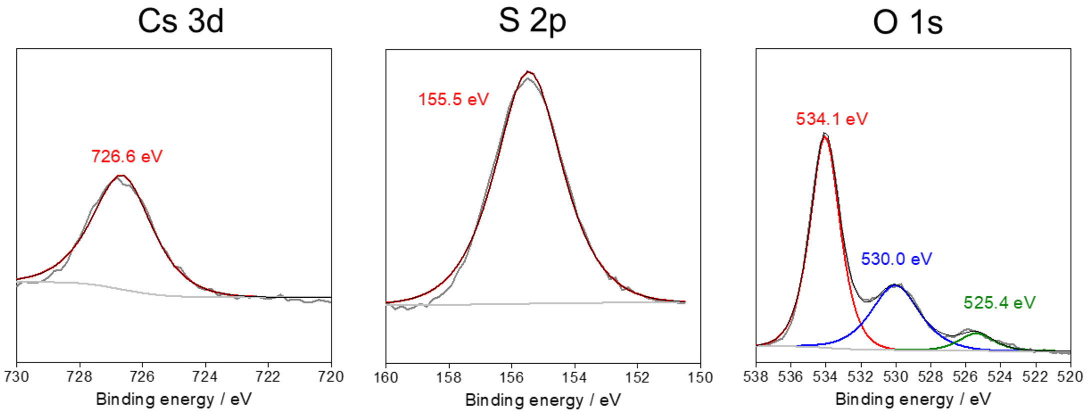

Figure S16. XPS spectra of Cs_2SO_4/SiO_2

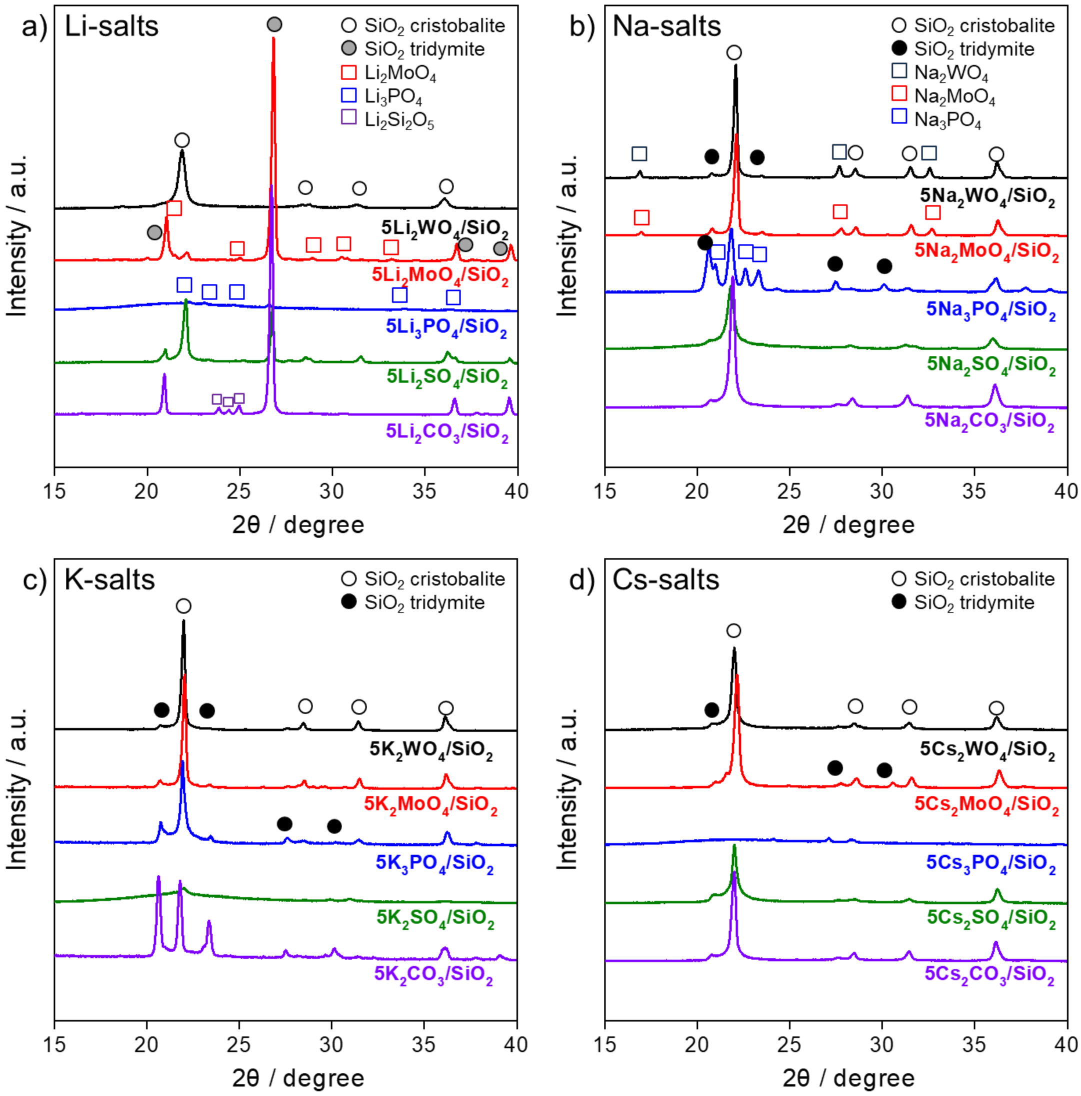

Figure S17. XRD profiles of (a) Li-salts, (b) Na-salts, (c) K-salts and (d) Cs-Salts on SiO_2.

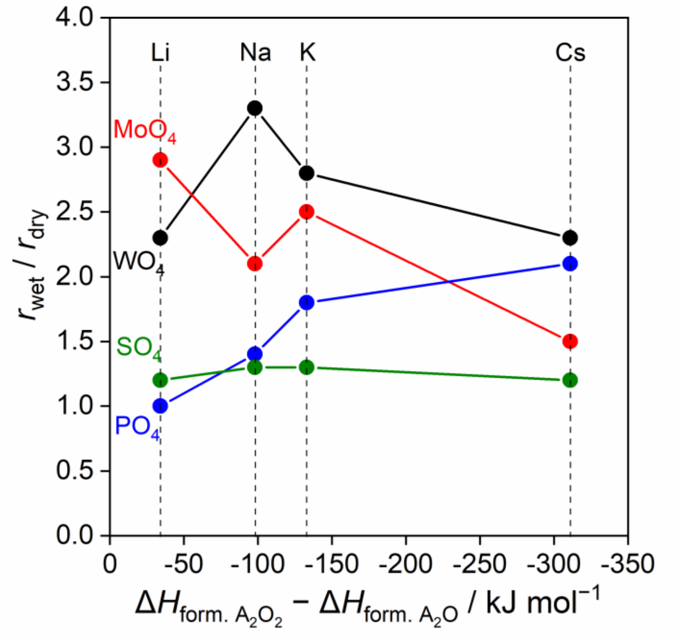

Figure S18. Ratio of wet (1.7 kPa H_2O added) over dry (no additional H_2O) CH_4 conversion rate as a function of enthalpy of reaction to form alkali metal peroxide (M_2O_2) from alkali metal oxide (M_2O). Rates taken at 1% CH_4 conversion and 850 °C with 10 kPa CH_4, 1.7 kPa O_2, and balance Ar.

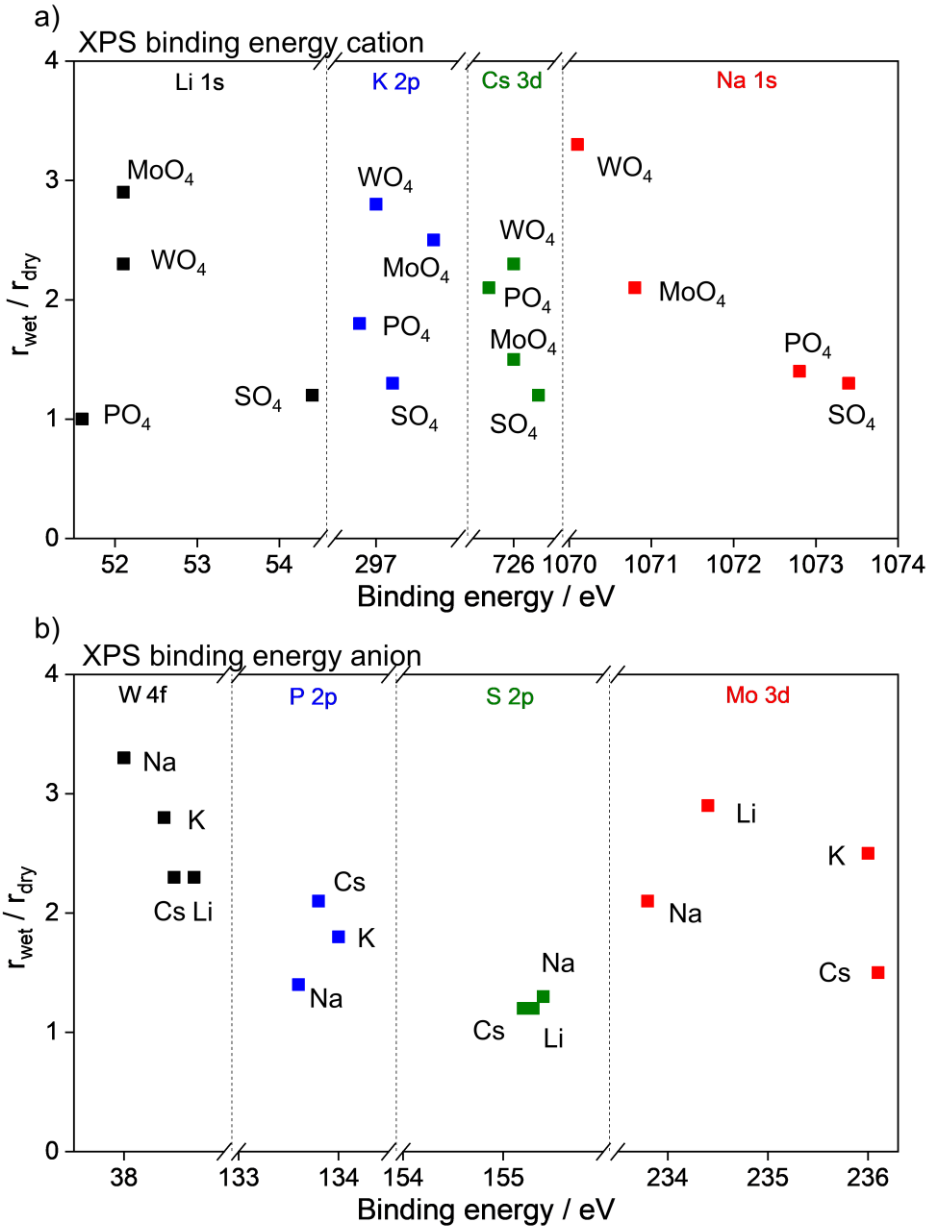

Figure S19. Value of $r_{\mathrm{wet}}/r_{\mathrm{dry}}$ as a function of XPS peak binding energy of a) cation species or b) anion centers.

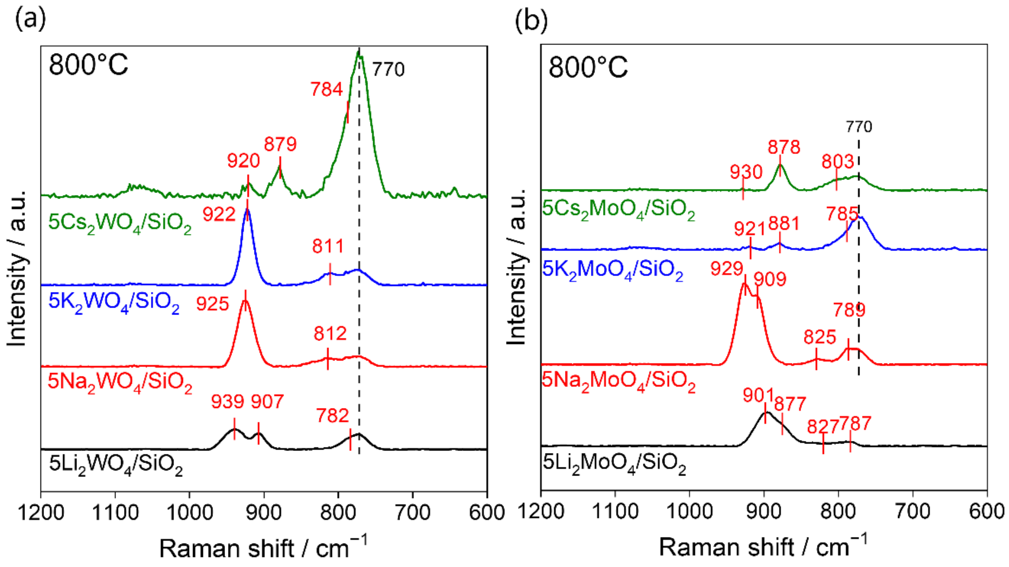

Figure S20. In-situ Raman of (a) WO$_4^{2-}$-related catalysts and (b) MoO$_4^{2-}$related catalysts.

References

1 R. Gupta, D. H. Kim and H. T. Kim, *Ceram. Int.*, 2022, **48**, 15282–15292.

2 H. Coker, *J. Phys. Chem.*, 1976, **80**, 2078–2084.

3 D. Zhou, C. A. Randall, H. Wang, L. X. Pang and X. Yao, *J. Am. Ceram. Soc.*, 2010, **93**, 1096–1100.

4 H. Kähäri, PhD thesis, University of Oulu, 2016.

5 X. Cs, X. Xue, Q. Csn, Z. Qi, H. Wang, Y. Zhao and J. Guo, *J. Eur. Ceram. Soc.*, 2023, **43**, 1477–1482.

6 H. Zhang, X. Wang, Q. Cheng, X. Ma, M. Cs, P. Zhang and Y. Zhao, *J. Mater. Sci.*, 2016, **27**, 5422–5426.

7 S. A. Abbas, I. Mahmood, M. Sajjad, N. A. Noor, Q. Mahmood, M. A. Naeem, A. Mahmood and S. M. Ramay, *Chem. Phys.*, DOI:10.1016/j.chemphys.2020.110902.

8 W. Zhen, S. Cs and B. Jianjiang, *Ceram. Int.*, 2013, **39**, 9767–9772.

9 D. Zhou, C. A. Randall, L. X. Pang, H. Wang, J. Guo, G. Q. Zhang, X. G. Wu, L. Shui and X. Yao, *J. Am. Ceram. Soc.*, 2011, **94**, 348–350.

10 X. Yuan, X. Xue and H. Wang, *J. Am. Ceram. Soc.*, 2019, **102**, 4014–4020.

11 J. Hao, J. Guo, C. Ma, F. Z. Yao, B. Yao, M. Si, E. Zhao and H. Wang, *J. Eur. Ceram. Soc.*, 2021, **41**, 6029–6034.